AFRL-RX-WP-TP-2009-4210

THE MEAN VS LIFE-LIMITING FATIGUE RESPONSE OF A Ni-BASE SUPERALLOY, PART 1: MECHANISMS (PREPRINT)

S.K. Jha, M.J. Caton, and J.M. Larsen

Metals Branch
Metals, Ceramics, and NDE Division

SEPTEMBER 2008

AIR FORCE RESEARCH LABORATORY
MATERIALS AND MANUFACTURING DIRECTORATE
WRIGHT-PATTERSON AIR FORCE BASE, OH 45433-7750
AIR FORCE MATERIEL COMMAND
UNITED STATES AIR FORCE

REPORT DOCUMENTATION PAGE

Form Approved
OMB No. 0704-0188

1. REPORT DATE *(DD-MM-YY)*	2. REPORT TYPE	3. DATES COVERED *(From - To)*
September 2008	Journal Article Preprint	

4. TITLE AND SUBTITLE
THE MEAN VS LIFE-LIMITING FATIGUE RESPONSE OF A Ni-BASE SUPERALLOY, PART 1: MECHANISMS (PREPRINT)

5a. CONTRACT NUMBER
In-house

5b. GRANT NUMBER

5c. PROGRAM ELEMENT NUMBER
62102F

6. AUTHOR(S)
S.K. Jha (Universal Technology Corporation)
M.J. Caton and J.M. Larsen (AFRL/RXLMN)

5d. PROJECT NUMBER
4347

5e. TASK NUMBER
RG

5f. WORK UNIT NUMBER
M02R3000

7. PERFORMING ORGANIZATION NAME(S) AND ADDRESS(ES)
Universal Technology Corporation
Dayton, OH 45432

Metals Branch (AFRL/RXLMN)
Metals, Ceramics, and NDE Division
Materials and Manufacturing Directorate
Wright-Patterson Air Force Base, OH 45433-7750
Air Force Materiel Command, United States Air Force

8. PERFORMING ORGANIZATION REPORT NUMBER
AFRL-RX-WP-TP-2009-4210

9. SPONSORING/MONITORING AGENCY NAME(S) AND ADDRESS(ES)
Air Force Research Laboratory
Materials and Manufacturing Directorate
Wright-Patterson Air Force Base, OH 45433-7750
Air Force Materiel Command
United States Air Force

10. SPONSORING/MONITORING AGENCY ACRONYM(S)
AFRL/RXLMN

11. SPONSORING/MONITORING AGENCY REPORT NUMBER(S)
AFRL-RX-WP-TP-2009-4210

12. DISTRIBUTION/AVAILABILITY STATEMENT
Approved for public release; distribution unlimited.

13. SUPPLEMENTARY NOTES
Journal article submitted to *Metallurgical and Materials Transactions*. PAO Case Number: 88ABW-2008-0114; Clearance Date: 09 Sep 2008.

14. ABSTRACT
The fatigue variability behavior of a powder metallurgy (P/M) Nickel-base superalloy, IN100, was studied from the perspective of the prediction of useful-lifetime. We found that stress level produced separate effects on the mean-fatigue behavior and the life-limiting mechanism. In the present IN100 material, this separation of responses is suggested to be related to the different levels of heterogeneity induced by the number density and the size distribution of constituent particles vs. those of voids, and by the sequence of selection of the failure modes. Furthermore, and perhaps of greater implication, in Part II we show that the life-limiting mechanism can be described in terms of the variability in small-crack growth from the relevant microstructural size. We also demonstrate that the above description of fatigue variability leads to a probabilistic life-prediction method based on crack growth, having the potential of significantly reducing the uncertainty in the lower-tail of fatigue variability, which is often described simply as the extrapolation of the deviation from the expected mean-response.

15. SUBJECT TERMS
fatigue variability, nickel-base superalloy, microstructure, life prediction, life-limiting mechanism, mean-dominating behavior, crack initiation, crack growth, probability of failure

16. SECURITY CLASSIFICATION OF:			17. LIMITATION OF ABSTRACT:	18. NUMBER OF PAGES	19a. NAME OF RESPONSIBLE PERSON (Monitor)
a. REPORT	b. ABSTRACT	c. THIS PAGE			James L. Larsen
Unclassified	Unclassified	Unclassified	SAR	32	19b. TELEPHONE NUMBER *(Include Area Code)* N/A

Standard Form 298 (Rev. 8-98)
Prescribed by ANSI Std. Z39-18

The Mean vs. Life-Limiting Fatigue Response of a Ni-Base Superalloy, Part I: Mechanisms

S. K. Jha[1], M. J. Caton, and J. M. Larsen

US Air Force Research Laboratory, AFRL/RXLMN, Materials and Manufacturing Directorate, Wright-Patterson Air Force Base, OH 45433, USA
[1]Universal Technology Corporation, Dayton, OH 45432, USA

ABSTRACT

The fatigue variability behavior of a powder metallurgy (P/M) Nickel-base superalloy, IN100, was studied from the perspective of the prediction of useful-lifetime. We found that stress level produced separate effects on the mean-fatigue behavior and the life-limiting (or worst-case) response. The observed fatigue variability behavior could therefore be described as the separation (or overlap) of mean-lifetime dominating mechanisms, and a life-limiting mechanism. In the present IN100 material, this separation of responses is suggested to be related to the different levels of heterogeneity induced by the number density and the size distribution of constituent particles vs. those of voids, and by the sequence of selection of the failure modes. Furthermore, and perhaps of greater implication, in Part II we show that the life-limiting mechanism can be described in terms of the variability in small-crack growth from the relevant microstructural size. We also demonstrate that the above description of fatigue variability leads to a probabilistic life-prediction method based on crack growth, having the potential of significantly reducing the uncertainty in the lower-tail of fatigue variability, which is often described simply as the extrapolation of the deviation from the expected mean-response.

KEYWORDS: Fatigue variability, Nickel-base superalloy, Microstructure, Life prediction, Life-limiting mechanism, Mean-dominating behavior, Crack initiation, Crack growth, Probability of failure

1. INTRODUCTION

The traditional approach to life management of fracture-critical turbine-engine components has been largely empirical in nature [1, 2]. Typically the decision for retirement is based on an extrapolation of the specimen "failure" (defined as the development of a predetermined level of damage) database for a range of tests to an acceptable probability of failure (taken as 1 in 1000, or the B0.1 lifetime). Due to a large degree of uncertainty associated with this approach, a majority of the components may be retired with a significant part of their useful lifetime remaining unutilized [1, 2]. One approach to this problem is to improve the accuracy of damage characterization to decrease the width of the "failure" lifetime distribution [3, 4]. A more significant impact on the uncertainty in life-prediction may, however, be realized by a paradigm shift in the description of fatigue variability itself towards a more physics-based theory [1]. In the present study, therefore, we seek to determine the physical basis of the uncertainty in fatigue-lifetime behavior and its dependence on microstructure and loading variables.

The fatigue variability behavior of superalloys has been studied by other researchers [5 - 12]. These materials are known to fail by crack initiation from processing related voids [5, 6, 9, 10, 13, 14], non-metallic constituent particles [11, 12-15], and from purely crystallographic crack initiation [11, 12]. Hyzak and Bernstein [5, 6] studied the effect of different types of constituent particles and voids on crack initiation with respect to temperature and strain amplitude. They reported a change in the crack initiation mode from the one controlled by constituent particles and voids at elevated temperature to crystallographic deformation at room temperature. Further, at elevated temperatures they observed the void-initiated failures at higher strain ranges and the constituent particle-related failures at lower strain ranges. They also found a transition strain level below which the failure initiation switched from the specimen surface to the subsurface.

This was attributed to crack initiation and crack growth dominated mechanisms at lower and higher strain ranges, respectively.

Several researchers have developed probabilistic descriptions of fatigue behavior of nickel-base superalloys [7 - 10] to predict the lifetime distribution. De Bussac and Lautridou [7] modeled failure from surface-inclusions or voids to obtain a distribution in lifetime with respect to the critical size of the controlling microstructural feature. In their work, the pores and the inclusions were treated equivalently in terms of their potential for failure initiation. Bruckner-Foit and coworkers [8] modeled the lifetime distribution for non-metallic inclusion initiated failures from a component surface. They included the variability in crack initiation as well as crack growth in their analysis. More recently, Luo and Bowen [9, 10] extended these models to incorporate the distribution in crack initiation and propagation from both pores and inclusions to describe the lifetime variability of a P/M nickel-base superalloy. They considered only the surface failure mechanism and treated pore and non-metallic inclusion equivalently [9, 10]. These models seem to describe the specific problem in each study well, although some authors acknowledge that the specific models may not address fatigue variability in the broadest sense.

The common aspects among the above studies can be listed as follows: (i) these tend not to account for the competition between different failure mechanisms at the same loading condition, and (ii) the sequence or the ranking of mechanisms in terms of their potential for causing failure is not addressed. One limitation of the above studies can be that these seem to be directed at determining the lifetime distribution from a given size distribution of microstructural feature. This has also been the emphasis of fatigue variability studies on other materials [16-18]. For this purpose, the material is often seeded to introduce a controlled level and size distribution of particles [11]. This is an important approach that provides useful insights into the lifetime-

variability, and in some cases [7, 9, 10] seeded defects may adequately represent the fatigue behavior. However, the typical approach to fatigue variability behavior has been to describe it as the distribution about the mean-lifetime behavior resulting from the deviation of input variables from their mean-values. Based on our study we argue that this conventional description of fatigue variability may overlook some very important differences between behaviors of the lower-tail vs. the mean lifetime with respect to these variables. Especially from a design-life perspective, a more encompassing problem appears to relate to the interplay between different degrees of microstructural heterogeneity and the process or the sequence of selection of mechanisms for given material characteristics and loading conditions. As we show later in this paper, the mean-behavior and the lower-tail or the worst-case behavior (which is more pertinent for life-prediction) may be driven by different mechanisms.

There are some studies that address the issues stated above. De Bussac [19] modeled the competition between surface and subsurface initiation in terms of the probability of finding the critical size feature at these locations, although no distinction was made between pore and inclusion related crack initiation. Also, the selection between the surface and the subsurface mechanism was invoked only on the basis of the inclusion or pore size, while the effect of the sequence of occurrence of failure mechanisms was not considered. For example, besides the inclusion / pore size considerations, the surface and the subsurface failures are sequential, and the former is expected to occur only if all conditions for the latter are not met. Todinov [20] recognized the ranking of the lifetimes of failure from different microstructural features and based his formulation of the cumulative lifetime distribution on this relationship between the various modes. A crack initiation probability was assigned to each group of features [20]. Yi and coworkers [21] in their study on a cast Al-Si alloy also performed a similar analysis that was

based on ranking of pores in terms of size ranges. An alternate approach can be to rank the mechanisms, rather than by average lifetime. Besides allowing for the effects of competing mechanisms, this will also account for the physically plausible case that two different mechanisms may produce similar lifetimes, although one may remain dormant unless the condition for the other is not experienced.

A recent paper, Jha, Larsen, and Rosenberger [22], shows that the microstructure and test conditions have separate and significantly different influences on the life-limiting vs. mean-fatigue behavior of an $\alpha+\beta$ titanium alloy. Chandran and Jha [23] modeled the competition between the surface and the subsurface failure in a beta titanium alloy by accounting for the different propensities of occurrence of the mechanisms. These and other studies [24, 25] indicate that an extrapolation of the variability about the mean behavior, while safe in most cases, may lead to excessively conservative design-life prediction in others. In the present study we address these issues with reference to the IN100 material and attempt to develop an improved understanding of the general fatigue variability behavior, especially in relation to the method of life prediction. Part I of the paper presents the concept of separate responses to stress level of the mean fatigue behavior vs. the life-limiting behavior and its relationship to sequential failures initiating from different scales of heterogeneity in IN100 is presented. In Part II, a life prediction method based on this description of fatigue variability is developed and discussed with a focus on increasing the reliability in predicted lifetimes.

2. MATERIAL AND EXPERIMENTAL PROCEDURE

Material

A powder-metallurgy processed and subsolvus-treated nickel-based superalloy, IN100, was examined in this study. The microstructure of the alloy, shown in Fig. 1, consisted of γ-phase grains and primary, secondary, and tertiary γ' precipitates. The γ - primary γ' structure is shown in Fig. 1(a). The secondary γ' morphology is revealed in Fig. 1(b). The tertiary γ', which are much finer, were not resolved at this magnification. The γ grain size distribution is shown in Fig. 1(c). As shown, the mode of the γ grain size distribution was at about 3 - 4 μm. In addition to these phases, the microstructure also contained non-metallic constituent particles and pores typical of powder processed superalloy materials [11, 12]. The size distribution and number-density of pores and the constituent particles were estimated based on an examination of about 100 mm^2 area of the material. The area number density of pores was estimated to be about 19/mm^2. The non-metallic particles (NMP) were relatively rare and their number-density was about 0.17/mm^2. The approximate volume densities could be derived following the formulations of Fullman [26] as adopted by Spowart, et. al. [27], and Yi and coworkers [21], and those were about 2445/mm^3 and about 10/mm^3, respectively, for the pores and the NMP. The size distributions of the pores and the NMP are shown in Fig. 2 (a) and (b), respectively. The lognormal probability density function provided a good description of the size distributions, as shown. On an average the NMP were slightly larger than the pores. However, due to the very low number-density of the NMP, only a limited number of constituent particle measurements could be made in the area examined, which produced some uncertainty with respect to the true NMP size distribution.

The 0.2% yield strength and the ultimate tensile strength of the material at the test temperature of 650°C were about 1100 and 1379 MPa, respectively. The elongation % at the same temperature was about 20%. The elastic modulus was about 186 GPa.

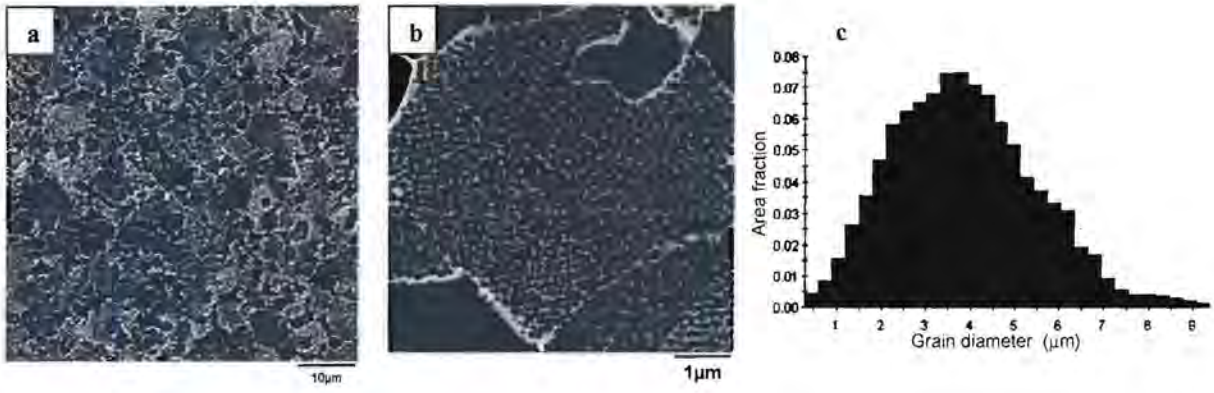

Figure 1: Microstructure of the IN100 material; (a) the γ and the primary γ' structure, (b) the secondary γ' morphology, and (c) the γ grain size distribution.

Experimental Procedure

The microstructure was characterized using a LEICA field-emission scanning electron microscope (SEM). The images were acquired at 15 KV accelerating voltage, with a beam current of 100 pA and a working distance of 15 mm. The γ-grain size distribution was determined by orientation imaging microscopy (OIM) scanning of a nominal area of the material using a TSL™ (a trademark of the EDAX Company) OIM camera and associated software. In order to determine the non-metallic particle and the pore size distributions, long-duration, high-resolution scans of several large areas were acquired in the SEM. The size distributions were measured using the ImagePro™ image analysis program.

The specimens tested in this study were extracted in the circumferential orientation from a pancake forging of the material. A cylindrical, button-head test specimen with a gage length of 15.2 mm and a diameter of 5 mm was used, as described in [28]. The specimens had a low-stress-ground (LSG) finish.

The fatigue tests were conducted using an MTS servo-hydraulic test system with a 646 controller. An electric resistance furnace was mounted on the test frame. A high-temperature button-head gripping assembly was used in conjunction with a standard collet-grip system to

transfer load to the sample. The hydraulic grip units were water-cooled. Temperature-control thermocouples were welded outside of the specimen gage section to maintain the test temperature at the specimen. The tests were performed in load control at a frequency of 0.33 Hz, a stress ratio (R) of 0.05, and a temperature of 650°C.

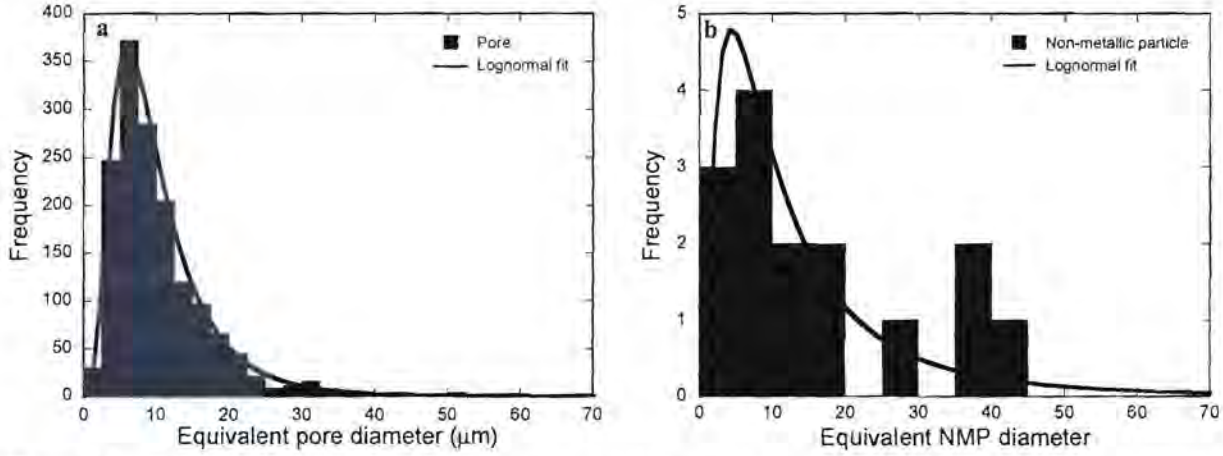

Figure 2: The size distribution of microstructural features in the IN100 alloy; (a) pore, and (b) non-metallic particle.

A high temperature extensometer was used to record the stress-strain behavior throughout the test. A typical stress-strain profile in the first 10 cycles and beyond at the stress level of 1150 MPa is presented in Fig. 3. As shown, there was tendency to strain-harden within the first few cycles. This hardening behavior was also observed at other stress levels. The strain ratcheting behavior can also be seen in Fig. 3.

The small-crack growth behavior was recorded using an acetate replication technique. The small-crack specimens were electropolished to remove surface damage and residual stress from machining. The replication tapes were examined in an Olympus^{TM} optical microscope for crack length measurements. The specimens were examined in a LEICA field emission Scanning Electron Microscope (SEM) upon fracture to document the crack- initiation and growth

characteristics. The crack initiation size was outlined in each sample and quantified using the ImagePro^{TM} image analysis program.

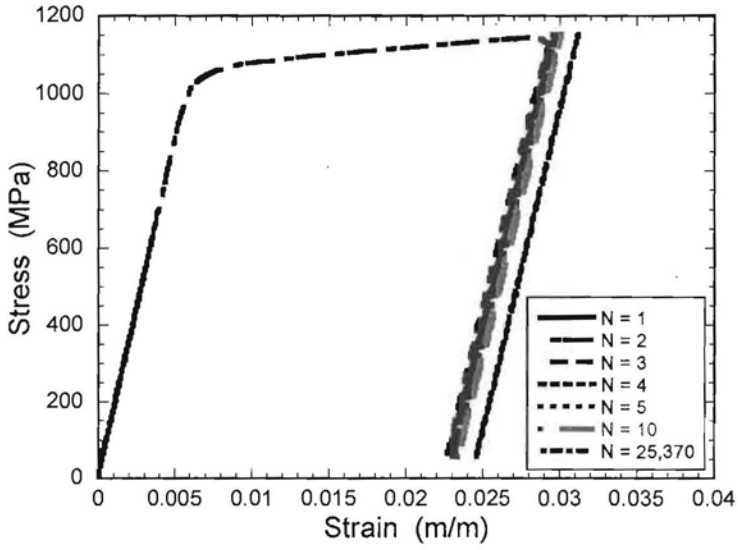

Figure 3: Typical stress-strain loop exhibited by IN100 under constant amplitude loading at σ_{max} = 1150 MPa.

3. RESULTS AND DISCUSSION

3.1 Fatigue Variability Behavior

The fatigue variability behavior of IN100 at 650°C is shown in Fig. 4 (a). As shown, while the mean-lifetime (illustrated by the dashed-line) and the life-limiting behavior tend to overlap at the highest stress level (1200 MPa), a separation between the two is seen at lower stress levels (σ_{max} = 1150 and 1100 MPa), such that the mean-lifetime is dominated by the more frequent and the longer-lifetime mechanism. This divergence of the mean behavior from the limiting response (as illustrated in Fig. 4(b)) resulted in an increase in the total variability with decreasing stress level. The fatigue variability behavior of IN100 can therefore be described as separation of a mean-dominating mechanism (or mechanisms) and a life-limiting mechanism as the stress level is decreased.

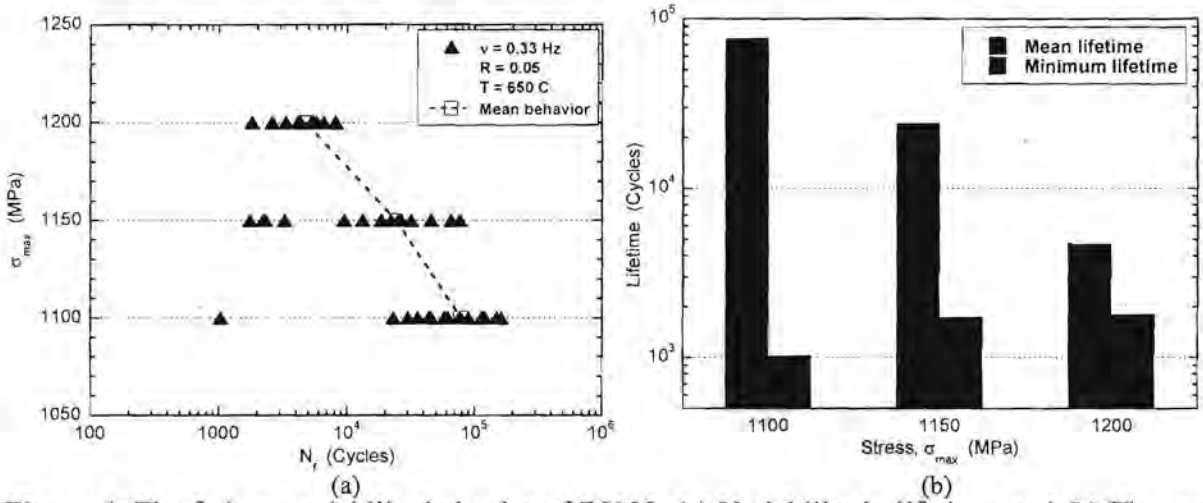

Figure 4: The fatigue variability behavior of IN100; (a) Variability in lifetime, and (b) The mean vs. the minimum lifetime with respect to stress level.

The conventional understanding driving material design for fatigue resistance [29] and useful-lifetime prediction [30] appears to be guided by the mean-fatigue behavior. For instance, in the conventional approach, the effect of changes in microstructure and external variables on the uncertainty in high cycle fatigue (HCF) lifetime is typically understood in terms of variability with respect to the expected mean-behavior [7, 9, 10, 30]. The underlying assumption is that, since the mean-lifetime is a strong function of microstructure and loading variables, the distribution in lifetime also follows the mean and can be calculated from deviations of these input variables from their mean values. This is clearly a valid description where the goal might be to affect only the average fatigue properties, but this approach may not facilitate the understanding of the relationship of the input variables to the tails of the response. The conventional description may therefore be inadequate, as it appears to not account for the probability of a response that does not follow the mean-fatigue dominating mechanism. In the present IN100 material, for example, the mean-lifetime and the life-limiting behavior respond differently to the stress level, causing separation between the trends for mean vs. minimum-life fatigue behavior (Fig. 4(a)). Therefore, although the mean-lifetime follows the expected response

to stress level, it may not be accurate to extrapolate the variability about the mean to determine the lower-tail behavior, for e.g., the B0.1 lifetime [25] which is used to determine design and service-life capability.

With respect to the above discussion, it is also useful to plot the experimental points in the cumulative distribution function (CDF) space, as shown in Fig. 5 (based on the lognormal probability density function (PDF)). While the CDF agreed well with the data at σ_{max} = 1200 MPa, the agreement was very poor at 1150 and 1100 MPa. A step-like shape of experimental points, illustrated by dashed lines, can be seen at σ_{max} = 1150 MPa. This indicates superposition of at least two mechanisms at that stress level, both of which contribute to the total variability [25]. Due to the single instance of the worst-case failure at 1100 MPa, the step-like behavior although physically plausible, is not yet revealed. The increase in uncertainty with decreasing stress level may, therefore, be related to this superposition of variability in the worst-case and the mean-dominating mechanism with diverging lifetimes.

Figure 5 also shows that the extrapolation of deviation with respect to the mean-behavior does not produce a consistent trend in the B0.1 lifetimes as a function of stress level. For example, a higher B0.1 lifetime is predicted at 1200 MPa, due to the decrease in the total variability, than at 1150 MPa. On the other hand, although a higher B0.1 lifetime is predicted at 1100 MPa, it is anticonservative with respect to the observed minimum lifetime, due to the CDF being heavily biased towards the mean behavior in this case. As we show in [22], such anomalous predictions of the probabilistic lifetime-limit can be resolved in the framework of separate responses of the lower-tail and the mean-dominating behavior to microstructure and loading variables.

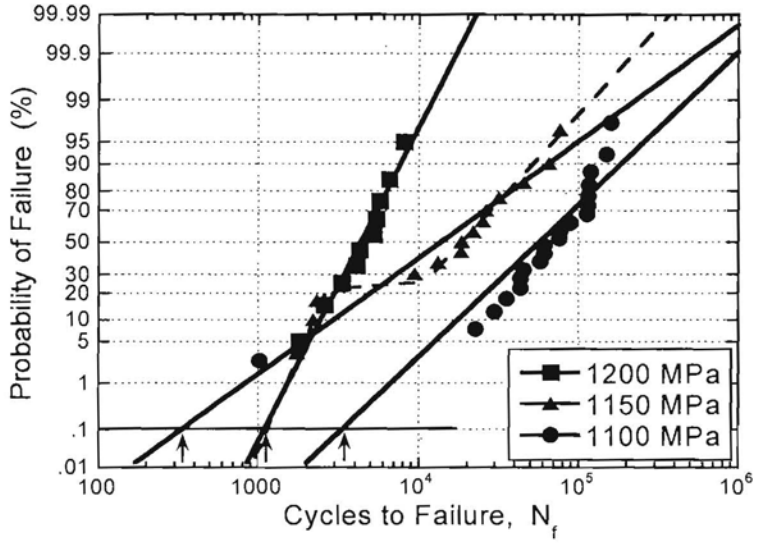

Figure 5: The experimental points plotted in the CDF space.

3.2 Competition between Mechanisms

Surface vs. Subsurface failures

The failures are characterized in terms of surface vs. subsurface crack initiation in Fig. 6(a). At the σ_{max} of 1200 MPa, the surface mechanism was observed exclusively. At the lower stress levels, however, a mix of surface and subsurface failures occurred, such that the probability of subsurface failures abruptly increased below σ_{max} = 1200 MPa. Clearly, the life-limiting distribution consisted of only the surface initiated failures. It should be noted that by surface failure we refer to crack initiation from a microstructural feature either intersecting the surface or just inside the surface (up to about one grain diameter). In the latter case, the ligament between the surface and the feature is thought to fail rapidly, such that the problem can essentially be treated as surface failure [31].

Crack initiation modes

In Fig. 6(b), the experimental points are identified in terms of the NMP vs. the pore-initiated failure. Comparing this with Fig. 6(a), samples can be classified into three failure mechanisms,

i.e., failures from (i) surface NMP, (ii) subsurface NMP, and (iii) surface pore. Examples of each of these mechanisms are presented in Fig. 7 (a), (b), and (c) respectively. The samples in Fig. 7 were tested at the same σ_{max} level of 1150 MPa. As shown in Fig. 6 (a) and (b), the life-limiting distribution was produced by failure from surface NMP. On the other hand, the mean-lifetime dominating distribution was composed of surface-pore and subsurface-NMP failures. It is also clear from Fig. 6 that all subsurface failures were initiated at NMP and all pore-initiated failures were in the surface. This can be related to the number densities of these features. A relatively large number density of pores may make the probability of a critical surface-pore related site close to unity. On the other hand, a very small number density of non-metallic particle may result in only a small probability of finding a critical non-metallic particle related site in the surface.

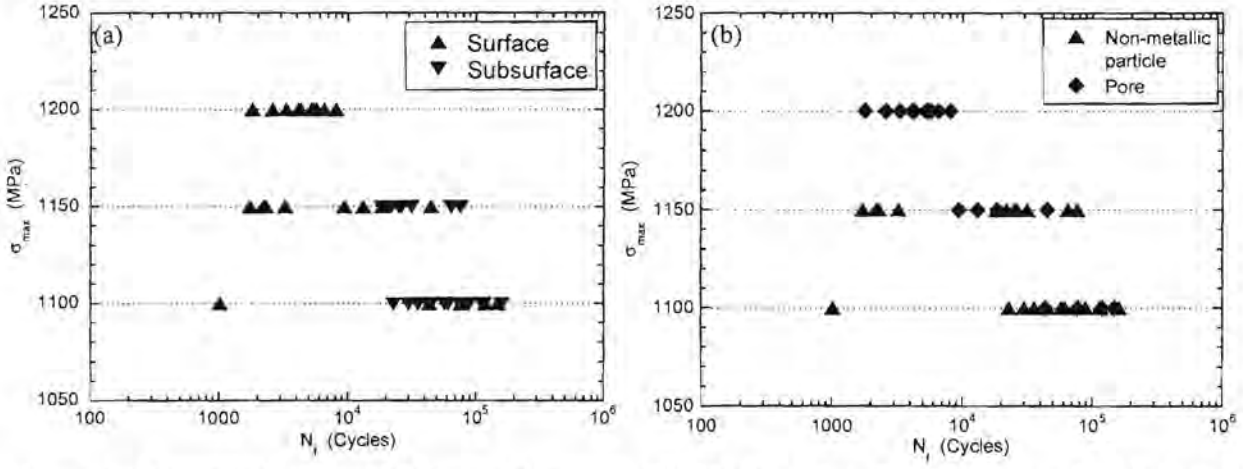

Figure 6: Characterization of fatigue failures in IN100; (a) subsurface vs. subsurface initiated failures, and (b) non-metallic particle vs. pore related failures.

Since the free surface and the region close to it experience a higher microplasticity level [32] than the bulk, especially at low nominal stress levels [32], the crack initiation is thought to be biased towards the surface. The distance of crack origin from the surface is shown with respect to lifetime in Fig. 8. For clarity, all surface failures have been plotted at d = 0 μm. As shown, the subsurface failures initiated anywhere from about 100 μm to about 2000 μm from the surface.

Besides the fact that the surface NMP initiated failures had smaller lifetimes, there was no apparent correlation between the crack initiation distance and the lifetime of subsurface-initiated failures.

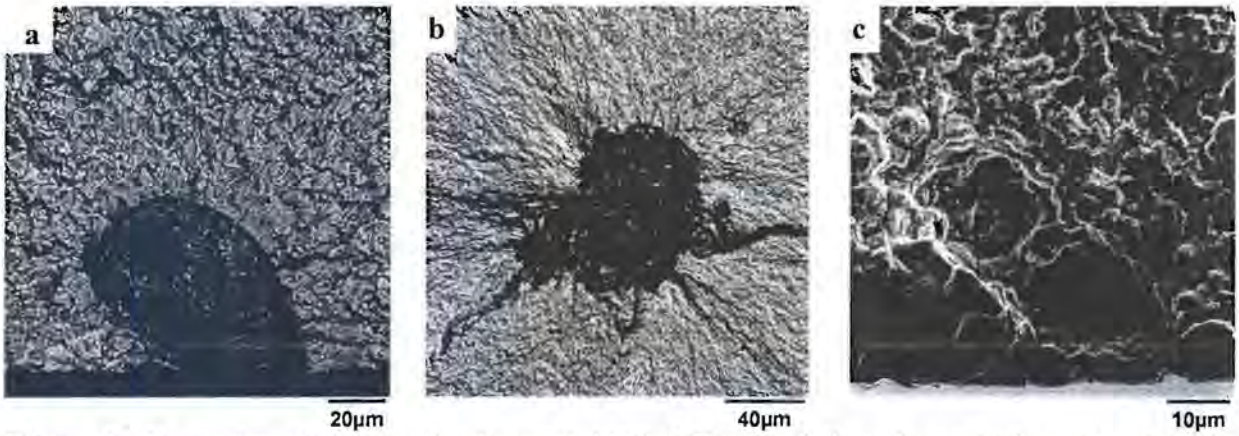

Figure 7: Examples of fatigue fractures at 1150 MPa; (a) failure from surface non-metallic particle, N_f = 2210 cycles, (b) failure from subsurface non-metallic particle, N_f = 25,081 cycles, and (c) failure from surface pore, N_f = 13,188 cycles. (a) and (b) are back scattered electron images and (c) is a secondary electron image.

The relationship between the crack initiation size (in terms of crack initiation area measured on a fracture surface) and lifetime is shown in Fig. 9. Firstly, it is clear that the crack initiating pores had smaller sizes than the non-metallic particles. This may partly explain the similar lifetimes of the surface-pore and the subsurface-particle failures in spite of the latter occurring in a pseudo vacuum condition. The range of crack initiation sizes for the worst-case failures, for example at 1150 MPa, was the same as that for the subsurface NMP failure. Therefore, for the particle-initiated failures, the separation into the worst-case and the mean-dominating distribution was not related to the size but to the location, i.e., surface or subsurface. It is also interesting to note the tendency towards larger failure-initiating non-metallic particles at the lower stress level (1100 MPa).

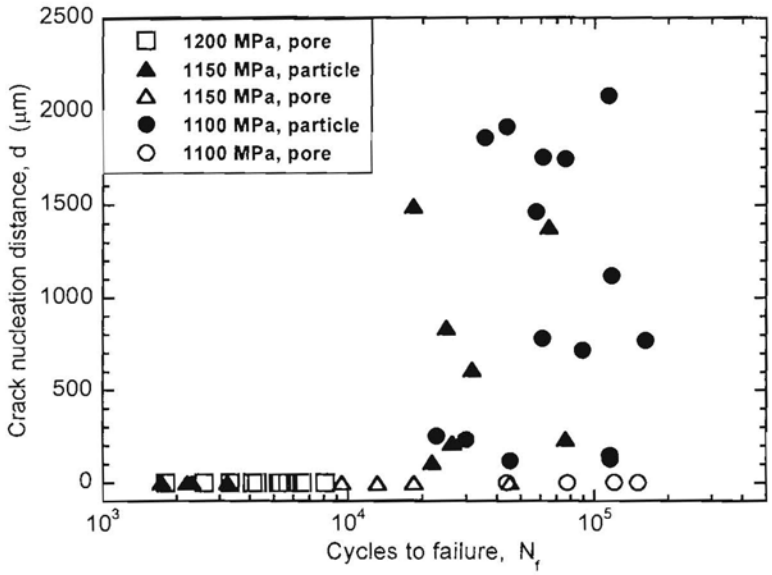

Figure 8: The crack initiation distance with respect to lifetime in IN100.

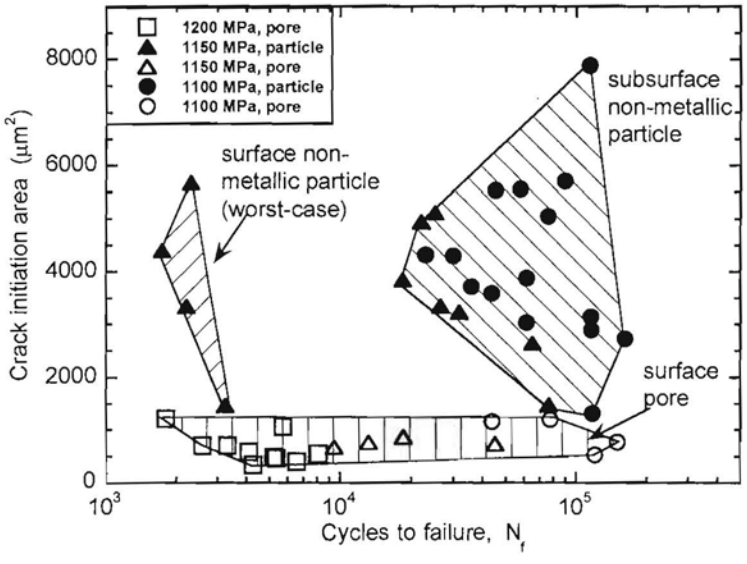

Figure 9: Crack initiation size – lifetime relationship in IN100 showing competition between mechanisms.

A comparison of the crack initiation size distribution for the NMP and the void-initiated failures vs. the nominal size distributions is made in Fig 10 (a) and (b), respectively, in order to study the relative size ranges critical for a given failure mechanism. For clarity, the y-axis has been normalized in this figure due to the difference in the number of features measured in a

nominal sample and the number of crack initiation size measurements. As expected, the crack initiation sizes were from the upper-tail of the nominal particle and pore size distributions, although there was no clear correlation between lifetime and crack initiation size. This is similar to earlier results by Tryon and coworkers [33] in another Ni-based material and could be due to the effect of the crack initiation neighborhoods in addition to the size [33] and to the small-crack growth variability. It is also evident that the critical NMP sizes tend to be much larger than the crack-initiating pore sizes.

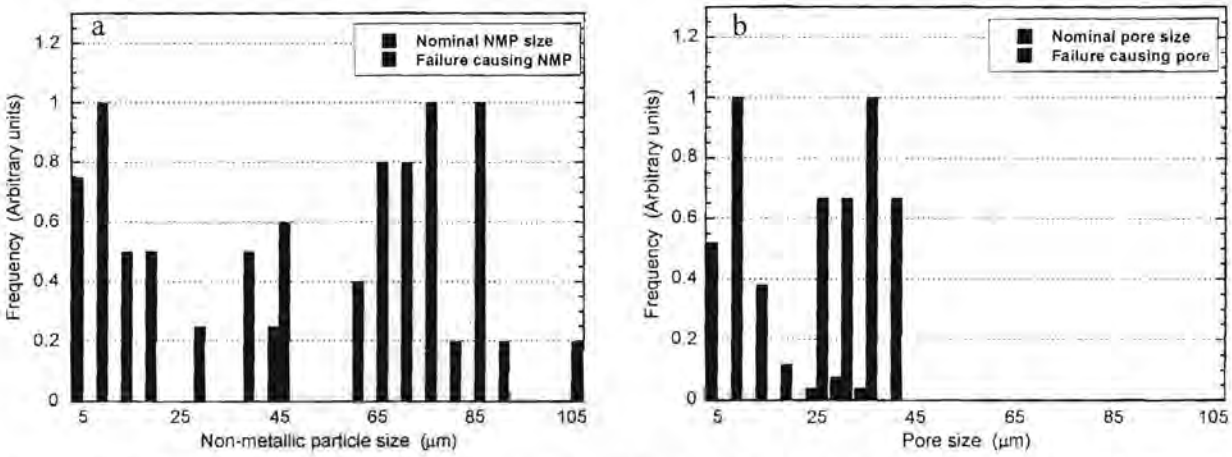

Figure 10: A comparison of the critical microstructure sizes to the nominal distributions; (a) Critical NMP sizes, and (b) critical pore sizes.

3.3 Ranking of Mechanisms

As discussed previously, the relative size distribution and the number density of microstructural features may produce different heterogeneity scales, affecting the probabilities and the order of selection of the mechanisms. This is suggested to produce the mean vs. the life-limiting effects on fatigue variability. It is important to recognize and understand these effects for not only reducing the uncertainty of life-prediction but also for the potential to increase reliability in the predicted useful lifetime. Here, by the "scale of heterogeneity" we imply the intensity of accumulated plastic deformation at the microscopic level. Analogies to some other

physical systems can be drawn here, for instance, second-order phase transition as a function of temperature in ferromagnetism [34] causing development of ordered domains or earthquake dynamics [35] which are believed to follow a power-law scaling in terms of intensity of shocks in any given geographic region [35] and progress at several size scales. The statistical-physics based concepts applied to these other fields may also provide clues towards understanding the fatigue variability behavior. A detailed discussion will be the subject of another paper.

Here, the ranking of mechanisms can be based on physical reasoning and experimental observation, as well as past experience with similar materials. As shown, stress level plays an important role in determining the separation / overlap of the mean-dominating and the life-limiting behavior. Other studies [22, 24] describe the influence of microstructure and temperature on this separation / overlap of mechanisms. The role of these variables can be understood in terms of their influence on the homogeneity (or heterogeneity) of deformation [36].

At higher stress levels, under relatively homogenized deformation, the mean and the life-limiting behavior can be thought to collapse and therefore indistinguishable from one another. As the stress level is decreased, different heterogeneity scales of local deformation may develop [37] and evolve in time [38], even in materials with no constituent particles or voids [38]. With reference to IN100, one scale of heterogeneity that may develop with decreasing stress level is the deformation around NMPs. It is known that, under some circumstances, a NMP is preferred over a pore of equivalent size as the failure initiation site [14, 39]. This is due to the stress field generated around a NMP as a result of elastic incompatibility with the matrix, and also the thermal expansion mismatch [14, 39, 40]. Clearly, this may not be the case in all materials depending on whether the NMP has higher or lower stiffness and the coefficient of thermal

expansion with respect to the matrix [40]. It is also known, that a NMP or pore in the surface has higher driving force for crack initiation and propagation than a feature of the same size in the subsurface [19, 23]. From these two statements it can be derived that a condition can exist where a subsurface NMP of relatively larger size may cause failure in preference to a surface pore. The very low number density of NMP makes it highly non-uniformly distributed in a sample when compared to the pores, hence a very low probability of occurrence of the surface NMP initiated mechanism.

It can be suggested that under relatively uniform deformation, a decrease in the driving force differential between failure from a NMP and that from a pore may be related to the decreased effect of elastic incompatibility and particle related residual stress field at higher applied stresses. Hyzak and Bernstein [6] suggested that this corresponds to the decrease in the crack initiation life differential between pore and NMP at higher stress levels. In that case, the sites of NMPs may not be distinguishable as a higher heterogeneity scale to cause the subsurface-particle (or surface-particle) mechanism in favor of the surface pore-initiated failure. This might be another explanation for the results by Hyzak and Bernstein [5, 6] and Gabb, et. al. in the NASA studies [11, 12]. Hyzak and Bernstein's work [5, 6] also indicated a critical strain level below which the failure mechanism shifted from surface pore to subsurface NMP, which is consistent with the above discussion. However, we did not see a sharp transition between pore vs. NMP-initiated failures (Fig. 5), meaning that there is some probability (at least in the theoretical sense) of each mechanism under all conditions. With a small number of tests, it is likely that only the mean-behavior is sampled at each stress level. Possibly, a "sufficient" number of trials would have revealed the more complete fatigue variability behavior, including contributions from surface NMP and surface-void related failures, even at lower stress levels [5, 6]. We recognize that the

"sufficient" number will be specific to a problem, depending on the size-distribution and number-density of the microstructural features, and may only be a theoretical possibility in some cases. In the least, it is crucial to develop a description of fatigue variability that provides a framework to assign probabilities to these effects. It is recognized that more work is required to resolve the stress-level effect on crack-initiation from NMP. The NASA study [11] has also recommended further experiments to understand the influence of temperature on failure initiation from a NMP.

Based on the above discussion, it is suggested that the ranking of crack initiating mechanisms should be in the sequential order of decreasing scale of the heterogeneity involved in a mechanism, but it may be difficult to develop such a ranking that is consistent across all stress levels. For example, in the present case and other studies [5, 6, 11], the failure from NMP may not be the most dominant mechanism at all stress levels. One relatively consistent approach can be to consider the uniformity of the distribution of a microstructural feature, which is related to the number-density of the feature. Therefore, in the present case the mechanisms can be ranked in the following order: (I) failure from surface NMP, (II) failure from subsurface NMP, and (III) failure from surface pores. As indicated previously, with increasing stress level the damage accumulation at a NMP may not be distinct enough from that at a pore to be critical for crack initiation. Therefore, the condition for occurrence of the NMP initiated failure may be absent in almost all samples at 1200 MPa (Fig. 5), leading to the last mechanism in the sequence, i.e., failure from surface pore. The observations at 1150 and 1100 MPa are also consistent with this sequence of mechanisms. Given the very small number density of NMPs and a significantly more uniform distribution of pores, the likely criteria for failure can be listed as:

(i) If a "critical" NMP is present in the surface, the sample fails from mechanism I, irrespective of whether or not the condition for mechanisms II and III are present.

(ii) If the criterion (i) is not met and a "critical" NMP is present in the subsurface, the sample fails from mechanism II, irrespective of whether or not the condition for mechanism III is present.

(iii) If both criterion (i) and (ii) are not met then the sample fails from mechanism III – failure from a surface pore.

Here by "critical" we imply the size necessary to cause the sufficient scale of heterogeneity for failure initiation for given microstructure and stress level. It should be noted that, for the purpose of discussion, we have ignored the effect of the neighboring matrix material at the pore and the NMP sites in determining the intensity of damage accumulation. However, the neighborhood effects are considered to play a very important role, as reported elsewhere [41].

If p_I, p_{II}, and p_{III} represent the probabilities for the occurrence of condition for mechanisms I, II, and III, respectively, then the cumulative probability of failure can be expressed as the sum of the probabilities of each mechanism [20, 21, 23]:

$$p_f = p_I + (1 - p_I)p_{II} + (1 - p_I)(1 - p_{II})p_{III} \quad (1)$$

If none of the three criteria is met, the sample is expected to fail by crystallographic crack initiation or not at all, within reasonable number of cycles. However, through simulation of the particle and the pore occurrence in a sample, given their size distribution and number densities [42], it can be shown that in the present IN100 material there is almost 100% probability of occurrence of a critical pore in the surface region. This, and the fact that the γ grain size distribution is much smaller than the pore sizes, makes it unlikely that the condition for surface pore failure will not be met in the present material. Eqn. 1 appears similar in form to the

expressions derived by Todinov in [20], and Yi and coworkers in [21], but the distinction here is that the probability of failure is based on the ranking of mechanisms as related to the underlying heterogeneity scales that exist at any given condition. Therefore, in spite of the almost 100% probability of crack initiation from a surface pore, mechanism III remains dormant (at lower stress levels) until the conditions for the higher ranking mechanisms are present in a sample. Also, mechanisms II and III produce similar lifetimes, but the former occurs in preference to the latter if the condition for it is present. The above criteria based on the ranking of mechanisms seem to account for these effects on fatigue variability.

The Source of Mean vs. Life-Limiting Behavior

As discussed above, the fatigue variability behavior seen here (Fig. 4) can be attributed to the relative number-densities and size-distributions of the microstructural features and the probabilities of occurrence of different scales of heterogeneity at a given stress level. However, this type of behavior is not limited to materials with constituent particles and pores. Even in materials with lower, or almost zero number-density of particles and pores, similar fatigue variability behavior was observed [22, 24, 43-45]. For example, in a supersolvus nickel-based superalloy with relatively larger γ grains and significantly lower pore content, the separation of lifetimes into mechanisms was related to crystallographic failure [24, 43]. In two microstructures of an α+β titanium alloy, such separation of the mean and the life-limiting response with decreasing stress level was seen to occur, seemingly due to finite probability of instant crack initiation from a particularly oriented equiaxed-α grain in certain lamellar α/β neighborhoods, even though the mean lifetime was clearly dominated by crack initiation [22]. We suggest that this might be the key factor driving the separation of the mean-dominating mechanism and limiting behavior with increasing material heterogeneity. This can be stated as being related to

the probability of a level of damage accumulation under any given loading condition that may cause relatively early failure-initiation, although the mean-lifetime is governed by a smaller-heterogeneity scale and therefore a relatively more uniformly distributed mechanism. Of course we recognize that in many cases such a probability can only be expressed in a theoretical sense and might be very difficult to observe experimentally, due to the large number of tests required.

4. CONCLUSIONS

The following primary conclusions can be drawn from this study:

(i) The mean and the life-limiting behavior of IN100 separated with decreasing stress level, producing an increase in the lifetime variability.

(ii) While the life-limiting behavior was related to failure by surface crack initiation from a non-metallic particle, the mean-dominating lifetime distribution consisted of a mix of failures from surface-void initiated and subsurface non-metallic particle initiated cracks.

(iii) A hierarchy of heterogeneity levels of local deformation is proposed to develop under any given microstructure and loading condition producing sequential mechanisms such that a probability of failure exists from a relatively higher-ranked but rare heterogeneity level defining the life-limiting behavior, while the mean-dominating behavior occurs from either a lower-ranked and more frequent heterogeneity scale or subsurface crack initiation.

REFERENCES

1. L. Christodoulou and J. M. Larsen, *JOM*, p. 15, March, 2004.

2. B. Cowles, *Mater. Sci. Engng.* Vol. A103, p. 63, 1988.

3. H. Ogi, M. Hirao, and S. Aoki, *J. App. Physics*, Vol. 1, p. 438, 2001.

4. J. D. Achenback, *Int. J. Solids and Struct.*, Vol. 37, pp. 13-27, 2000.

5. J. M. Hyzak, and I. M. Bernstein, *Metall. Trans.*, Vol. 13A, p. 33, 1982.

6. J. M. Hyzak, and I. M. Bernstein, *Metall. Trans.*, Vol. 13A, p. 45, 1982.

7. A. de Bussac, and J. C. Lautridou, *Fatigue Fract. Engng. Mater. Struct.*, Vol. 16, p. 861, 1993.

8. A. Bruckner-Foit, H. Jackels, and U. Quadfasel, *Fatigue Fract. Engng. Mater. Struct.* Vol. 16, p. 891, 1993.

9. J. Luo, and P. Bowen, *Acta Materialia*, Vol. 51, p. 3521, 2003.

10. J. Luo, and P. Bowen, *Acta Materialia*, Vol. 51, p. 3537, 2003.

11. T. P. Gabb, J. Telesman, P. T. Kantzos, P. J. Bonacuse, and R. L. Barrie, *NASA/TM-2002 211571*, 2002.

12. T. P. Gabb, P. J. Bonacuse, L. J. Ghosn, J. W. Sweeny, A. Chatterjee, and K. A. Green, *NASA/TM-2000-209418*, 2000.

13. D. Eylon and J. M. Hyzak, *Metall. Trans.*, Vol. 9A, p. 127, 1978.

14. D. A. Jablonski, *Materials Sci. Engng.*, Vol. 48, p. 189, 1981.

15. E. S. Huron and P. G. Roth, In: *Superalloys 1996*, 1996.

16. P. J. Laz and B. M. Hillberry, *Int. J. Fatigue*, Vol. 20, p. 263, 1998.

17. E. A. DeBartolo and B. M. Hillberry, *Int. J. Fatigue*, Vol. 23, p. S79, 2001.

18. S. Tanaka, M. Ichikawa, and S. Akita, *Engng. Fract. Mechanics*, Vol. 20, p. 501, 1984.

19. A. de Bussac, *Fatigue Fract. Engng. Mater. Struct.*, Vol. 17, p. 1319, 1994.

20. M. T. Todinov, *Computers and Structures*, Vol. 79, p. 313, 2001.

21. J. Z. Yi, Y. X. Gao, P. D. Lee, H. M. Flower, and T. C. Lindley, *Metall. Mater. Trans.*, Vol. 34 A, p. 1879, 2003.

22. S. K. Jha, M. J. Caton, and J. M. Larsen, *Mater. Sci. Engng. A*, Vol. 468-470, pp. 23-32, 2007.

23. K. S. Ravi Chandran and S. K. Jha, *Acta Materialia*, Vol. 53, p. 1867, 2005.

24. S. K. Jha, J. M. Larsen, and A. H. Rosenberger, *Acta Materialia*, Vol. 53, p. 1293, 2005.

25. S. K. Jha, J. M. Larsen, A. H. Rosenberger, and G. A. Hartman, *Scripta Materialia*, Vol. 48, pp. 1637-1642, 2003.

26. R. L. Fullman, *Trans. AIME*, Vol. 197, p. 447, 1953.

27. J. E. Spowart, B. Maruyama, and D. B. Miracle, *Mater. Sci. Engng.*, Vol. A307, p. 51, 2001.

28. S. K. Jha, M. J. Caton, J. M. Larsen, and A. H. Rosenberger, In: *Materials Damage Prognosis*, J. M. Larsen, et. al. Eds, TMS Publ., pp. 343-350, 2004.

29. K. S. Chan and M. P. Enright, *Met and Mater. Trans. A*, Vol. 36A, p. 2621, 2005.

30. R. Tryon and A. Dey, *J. Aerospace Engng.*, Oct 2001, pp. 120, 2001.

31. A. Borbely, H. Mughrabi, G. Eisenmeier, and W. H. Hoppel, *Int. J. Fracture*, Vol. 115, p. 227, 2002.

32. M. Sauzay, and P. Gilormini, *Fatigue Fract. Engng. Mater. Struct.*, Vol. 23, p. 573, 2000.

33. R. G. Tryon, A. Dey, G. Krishnan, K. S. R. Chandran, and M. Oja, in Materials Damage Prognosis, J. M. Larsen, L. Christodoulou, J. R. Calcaterra, et. al. Eds., TMS Publ., p. 105, 2004.

34. K. H. Hoffman and M. Schreiber, Eds., Computational Statistical Physics, Springer Publ., pp.211-226, 2002.

35. J. B. Rundle, D. L. Turcotte, R. Shcherbakov, W. Klein, and C. Sammis, *Review of Geophysics*, Vol. 41, pp. 1019, 2003.

36. V. P. Bennet and D. L. McDowell, *Int. J. Fatigue*, Vol. 25, pp. 27-39, 2005.

37. O. B. Pedersen, *Acta Metall. Materialia*, Vol. 38, pp. 1221-1239, 1990.

38. X. Feaugas and M. Clavel, *Acta Materialia*, Vol. 45, pp. 2685-2701, 1997.

39. M. M. Shenoy, R. S. Kumar, and D. L. McDowell, *Int. J. Fatigue*, Vol. 27, p. 113, 2005.

40. R. Bullough and L. C. Davis, *Acta Materialia*, Vol. 43, p. 2737, 1995.

41. M. Liao, *Symposium on Materials Damage Prognosis and Life Cycle Engng.*, Snowmass, CO, July, 2006.

42. S. K. Jha, M. J. Caton, J. M. Larsen, and A. H. Rosenberger, unpublished work, AFRL.

43. S. K. Jha, J. M. Larsen, and A. H. Rosenberger, *JOM*, p. 50, Sep 2005.

44. S. K. Jha, J. M. Larsen, and A. H. Rosenberger In: Fatigue 2006, International Fatigue Congress, Atlanta, GA, 2006.

45. M. J. Caton, S. K. Jha, J. M. Larsen, and A. H. Rosenberger, In: Superalloys 2004, p. 305, 2004.